Charge-dependent directed flow in asymmetric nuclear collisions

V. Voronyuk,[1,2] V. D. Toneev,[3] S. A. Voloshin,[4] and W. Cassing[5]
[1]*Joint Institute for Nuclear Research, Dubna, Russia*
[2]*Bogolyubov Institute for Theoretical Physics, Kiev, Ukraine*
[3]*Joint Institute for Nuclear Research, RU-141980 Dubna, Moscow Region, Russia*
[4]*Wayne State University, Detroit, Michigan, USA*
[5]*Institute for Theoretical Physics, University of Giessen, Giessen, Germany*
(Received 8 October 2014; revised manuscript received 18 November 2014; published 8 December 2014)

The directed flow of identified hadrons is studied within the parton-hadron-string-dynamics (PHSD) approach for the asymmetric system Cu + Au in noncentral collisions at $\sqrt{s_{NN}} = 200$ GeV. It is emphasized that due to the difference in the number of protons of the colliding nuclei an electric field emerges, which is directed from the heavy to the light nucleus. This strong electric field is only present for about 0.25 fm/c at $\sqrt{s_{NN}} = 200$ GeV and leads to a splitting of the directed flow v_1 for particles with the same mass but opposite electric charges in case of an early presence of charged quarks and antiquarks. The microscopic calculations of the directed flow for $\pi^{\pm}, K^{\pm}, p$, and $\bar{p}$ are carried out in the PHSD by taking into account the electromagnetic field induced by the spectators as well as its influence on the hadronic and partonic quasiparticle trajectories. It is shown that the splitting of the directed flow as a function of pseudorapidity η and in particular as a function of the transverse momentum p_t provides a direct access to the electromagnetic response of the very early (nonequilibrium) phase of relativistic heavy-ion collisions and allows us to shed light on the presence (and number) of electric charges in this phase.

DOI: 10.1103/PhysRevC.90.064903 PACS number(s): 25.75.Ag, 25.75.Ld, 24.10.Lx

I. INTRODUCTION

An important tool to probe the hot, dense matter created in heavy-ion collisions is the study of the particle azimuthal angular distribution in momentum space with respect to the reaction plane [1,2]. In high-energy nuclear collisions the energy density reaches values above 1 GeV/fm^3 at which the quantum chromodynamics (QCD)—the theory of the strong interactions—predicts a phase transition from normal hadronic matter to a deconfined state of quarks and gluons, the quark-gluon plasma (QGP). By now, a large amount of experimental data has been obtained at the relativistic-heavy-ion collider (RHIC) and the large-hadron collider (LHC) on the properties of strongly heated and highly compressed matter what allows to extract information on the equation of state of the excited matter as well as on the transport properties of the partonic degrees of freedom. However, the detailed properties of this new phase are still far from being fully understood.

A large elliptic flow v_2 of charged hadrons, observed at RHIC, testifies to the collective nature of the strong interaction at high energies. As the analysis shows [1,2], the excited matter behaves like a colored almost perfect liquid [3] [the so-called strongly coupled QGP (sQGP)] rather than a weakly interacting parton gas. The elliptic flow has been measured by many collaborations at energies from the alternating gradient synchrotron (AGS) to the LHC and the scaling properties of flow harmonics, their dependence on centrality, rapidity, and particle species have been studied. Higher harmonics, $v_n (n > 2)$, have been also intensively explored especially in recent years, when it became clear that odd harmonics are sensitive to fluctuations in the initial conditions. It finally turns out that the study of azimuthal asymmetries is closely related to structures in two-particle correlations of hard and semihard processes in the partonic phase [2].

In more recent times much attention has been paid again to the directed flow [4,5] of identified particles and the precise STAR measurements performed within the beam energy scan (BES) program in the energy range $\sqrt{s_{NN}} = 7.7$–39 GeV [6] have received a large amount of attention. The directed flow refers to a collective sideward deflection of particles and is characterized by the first-order harmonic v_1 of the Fourier expansion of the particle azimuthal angular distribution with respect to the reaction plane. An analysis [7] of these data within the microscopic PHSD transport approach and the collective three-fluid dynamics (3FD) model reproduces the general trend in the differential $v_1(y)$ excitation function and leads to an almost quantitative agreement especially at higher energies where the partonic phase is dominant. We recall that 3FD hydrodynamics [8] shows a high sensitivity to the nuclear equation of state (EoS) and provides the best results employing a crossover for the quark-hadron phase transition in the model. Note also that a crossover transition is implemented by default in the PHSD approach. This flow analysis has shown no indication of a first-order phase transition [7] as anticipated long before [9,10]. In all cases mentioned above only symmetric nuclear collisions have been considered. The most important parameters being varied in these analyses are the collision energy, the size of the system, and the centrality of the collision.

An additional insight into the mechanism of particle production in relativistic heavy-ion collisions and the electromagnetic response for very early times can be gained from interactions of nuclei with different sizes, e.g., Cu + Au collisions at the top RHIC energy of $\sqrt{s_{NN}} = 200$ GeV. The study of the charged hadron multiplicity distributions and correlations in the longitudinal direction for asymmetric collisions gives additional constraints to the mechanism of the energy deposition in the early stage of the reaction [11–14] by exploiting the particle asymmetry in pseudorapidity. Also, global characteristics of the directed flow are of substantial interest [15–17]. But it is more important, as expected in Refs. [18,19], that the directed flow in asymmetric collisions may be partly generated by a specific source. An electric field, arising from the difference in charges of the colliding nuclei, may lead to a nonzero contribution to the directed flow of charged particles and possibly could be disentangled by measuring the directed flow of particles with equal mass but opposite electric charge. Furthermore, one might have direct access to the positive and negative initial charge density by measuring charge differential flow. In this respect it is of great interest to compare the v_1 rapidity/pseudorapidity dependencies and transverse momentum dependence for identified hadrons that differ by the electric charge, v_1^+ and v_1^-, and to provide quantitative predictions for the differential observables.

Very recently, asymmetric Cu + Au collisions have been performed at RHIC and the directed flow for identified particles has been measured by the PHENIX Collaboration [14,20,21]. In Cu + Au collisions, a substantial electric field directed from a colliding Au nucleus to the Cu nucleus is generated in the overlap region (see below). This happens only when the colliding two nuclei carry a different number of electric charge. This electric field will induce an electric current in the matter created after the collision, resulting in a dipole deformation of the charge distribution. The time evolution of the system is known to be dominated by the strong radial flow, which is an outward collective motion of the medium. Henceforth the charge asymmetry formed in the early stage is frozen. Thus, it is argued that the charge-dependent directed flow of the observed hadrons is sensitive to the charge dipole formed at the early stage [22], which reflects the electric conductivity of the QGP [23] at early times. In symmetric collisions some other charge splitting may appear, its magnitude appears to depend strongly on the actual distance between the pion emission site and the spectator system and bring new, independent information on the space-time evolution of pion production [24].

We briefly recall that the early magnetic field eB_y [25] also may lead to the induction of charged currents in the system. These currents result in a charge-dependent directed flow that is odd in rapidity and odd under charge exchange and has to be added to the effects studied in this work due to the electric field eE_x.

The goal of this paper is the study of the charge-dependent directed flow in terms of the PHSD model for a quantitative specification/prediction of the v_1 splittings to be expected in two different scenarios. We will consider the production of π^+,π^-,K^+,K^- mesons and $p,\bar{p}$ baryons in Cu + Au collisions at $\sqrt{s_{NN}} = 200$ GeV taking into account the retarded electromagnetic field that is created dominantly by the proton spectators in the very early collision [26]. As primary observables we will address the differential directed flow $v_1(\eta,p_t)$ of these hadrons and explore the experimental perspectives.

II. REMINDER OF THE PHSD MODEL

The dynamics of partons, hadrons, and strings in relativistic nucleus-nucleus collisions is treated within the parton-hadron-string-dynamics (PHSD) approach. The PHSD model is a covariant dynamical approach for strongly interacting systems formulated on the basis of Kadanoff-Baym equations [28,29] or off-shell transport equations in phase-space representation, respectively. In the Kadanoff-Baym theory the field quanta are described in terms of dressed propagators with complex self-energies. Whereas the real part of the self-energies can be related to mean-field potentials of Lorentz scalar, vector, or tensor type, the imaginary parts provide information about the lifetime and/or reaction rates of timelike particles [30]. Once the proper complex self-energies of the degrees of freedom are known, the time evolution of the system is fully governed by off-shell transport equations for quarks and hadrons (as described in Refs. [28,30]). The PHSD model includes the creation of massive quarks via hadronic string decay—above the critical energy density $\varepsilon_c \approx 0.5$ GeV/fm^3—and quark fusion forming a hadron in the hadronization process. With some caution, the latter process can be considered as a simulation of a crossover transition since the underlying equation of state (EoS) in PHSD is a crossover [30]. At energy densities close to the critical energy density ε_c, the PHSD describes a coexistence of the quark-hadron mixture. This approach allows for a simple and transparent interpretation of lattice QCD results for thermodynamic quantities as well as correlators and leads to effective strongly interacting partonic quasiparticles with broad spectral functions. For a review on off-shell transport theory we refer the reader to Ref. [30]; PHSD model results and their comparison with experimental observables for heavy-ion collisions from the lower super-proton-synchrotron (SPS) to RHIC energies can be found in Refs.[30–33]. In the hadronic phase, i.e., for energies densities below the critical energy density ε_c, the PHSD approach is identical to the hadron-string-dynamics (HSD) model [34–36].

In the PHSD the initial kinetic energy is converted in hard nucleon-nucleon collisions to stringlike configurations via PYTHIA 6.4 and these strings decay to partonic quasiparticles with spectral functions in line with the dynamical quasiparticle model (DQPM, see Ref. [30]) if the energy density is above critical ($\approx$0.5 GeV/fm^3). The initial conversion of energy happens during roughly 0.15 fm/c at the top RHIC energy when the nuclei pass though each other. At this time the energy density in between the leading baryons is very high due to the fact that the spacial volume is very small as $\sim 0.3^3$ fm^3 in longitudinal extension; the transverse contribution to this volume is given by the overlap area. Due to the Heisenberg uncertainty relation this energy density cannot be specified as being due to particles since the latter may form only much later on a timescale of their inverse transverse mass (in their rest frame). More specifically, only jets at midrapidity with transverse momenta above $p_T = 2$ GeV are expected to appear at $t \approx 0.1$ fm/c while a soft parton with transverse momentum $p_T = 0.5$ GeV should be formed after $t \geqslant 0.5$ fm/c. Although it is not clear what the actual nature of the degrees of freedom is in this initial state, there will naturally be a small number of electric charges due to charge conservation. On the other hand, if a large number of electric charges (from the conversion of energy to quarks and antiquarks) are present in the very beginning of the reaction, then there should be observable signals from this early electric accelerator. It is our aim to

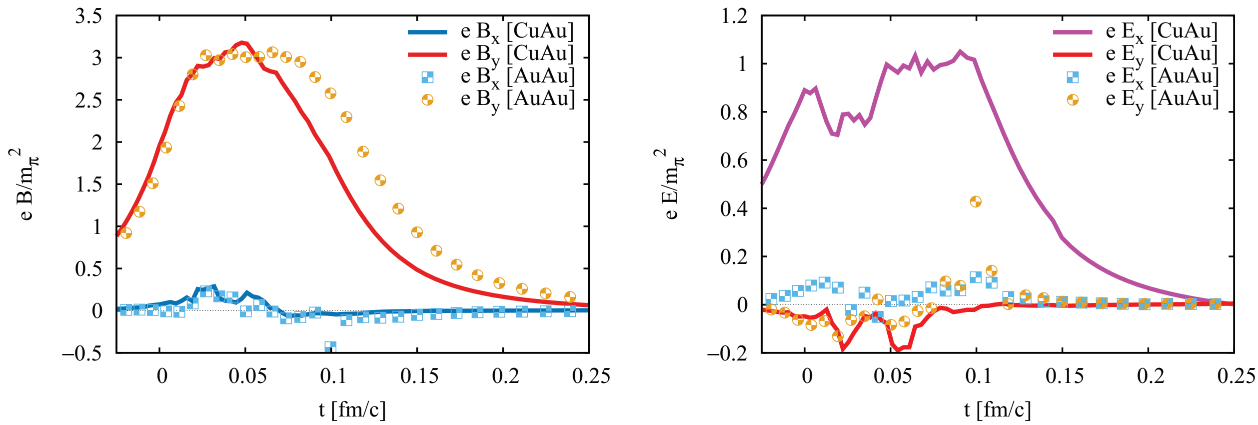

FIG. 1. (Color online) Time evolution of event-averaged components of the magnetic (left-hand side) and electric (right-hand side) fields in the center of the overlap region of colliding Cu + Au (solid lines) and Au + Au (dotted lines) systems at $\sqrt{s_{NN}} = 200$ GeV and $b = 7$ fm. The distributions are averaged over 70 events.

quantify within PHSD these possible signals and to provide robust predictions.

We use here the PHSD version where the creation of electromagnetic fields and particle transport in these fields are taken into account by means of the retarded Liénard-Wiechert potentials [26]. Only the source of the spectator protons is considered since this source is dominant at the initial stage when target and projectile spectators are close to each other. By the time of about 1 fm/c, after contact of the nuclei, the electromagnetic fields drop down by three orders of magnitude and become comparable with the field from the participants [26]. This offers the very specific property of the early electric field to check experimentally if electric charges are already present at this instant.

The time evolution of transverse electromagnetic field components is compared between asymmetric Cu + Au (solid lines) and symmetric Au + Au systems (dotted lines) in Fig. 1 where the left-hand side displays the magnetic field components and the right-hand side the electric ones. The maximal values of the magnetic field components $\langle eB_y \rangle$ are on the level of a few m_π^2 being comparable for both systems. For the symmetric case the results are in agreement with our earlier results in Ref. [26]. The electric field components also agree with the earlier results for symmetric collisions [26] but in the case of the Cu + Au reaction the $\langle eE_x \rangle$ component is by a factor of ∼5 larger than that for symmetric Au + Au collisions at the same energy [26]. This strong electric field eE_x is only present for about 0.25 fm/c during the overlap phase of the heavy ions and will act as an electric accelerator on charges that are present during this time. Note that when charges appear only later together with the formation of soft partons ($t \geqslant 0.5$ fm/c) there will be no corresponding charge separation effect on the directed flow. In the case of symmetric collisions it was noted that $\langle E_x \rangle \approx \langle B_y \rangle$ [26,37]. This approximate equality is broken for asymmetric Cu + Au collisions where $\langle eB_y \rangle > \langle eE_x \rangle$.

Figure 2, furthermore, shows the distribution in the strength and direction of electric field components for off-central Cu + Au and Au + Au collisions. This snapshot is made for the time when both nuclear centers are in the same transverse plane. This condition corresponds to different times for the two systems considered, which is confirmed by a shift of the

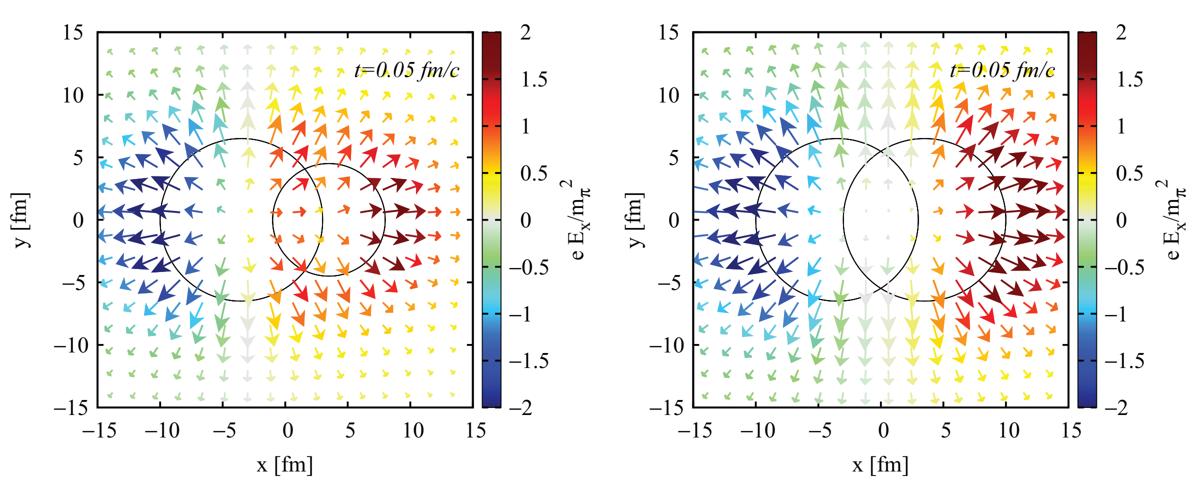

FIG. 2. (Color online) Event-averaged electric field in the transverse plane for a Cu + Au (left) and Au + Au (right) collision at 200 GeV at time $t = 0.05$ fm/c for the impact parameter $b = 7$ fm. Each vector represents the direction and magnitude of the electric field at that point.

component $\langle eB_y \rangle$ in time (cf. left-hand side of Fig. 1) where the maximum is reached earlier in Cu + Au collisions. Here we take $t \sim 0.05$ fm/c in view of Fig. 1. Note that in Cu + Au collisions a significant electric field eE_x is generated in the overlap region of the two nuclei in x direction, i.e., directed towards the lighter copper nucleus. The situation is different in collisions of nuclei of the same size [26,37,38] as illustrated in Fig. 2 (right-hand side). In symmetric collisions like Au + Au or Cu+Cu, the event-averaged electric field does not show a preferential direction and the magnitude of the electric fields generated in each event is lower, too.

This strong electric field eE_x towards the Cu nucleus at the early stage induces an electric current in the medium (if electric charges are present). As a result, the charge distribution is modified and a charge dipole is formed [22]. In central Cu + Au collisions the Cu nucleus is completely embedded within the Au nucleus and due to the absence of Cu spectators no sizable electric current is formed. We note in passing that the electric field sharply drops after $t \gtrsim 0.25$ fm/c in free space, while in conducting matter the time dependence of the field strength is flattening out and reaches some plateau even up to $t \sim 10$ fm/c [39]. The level of this plateau is proportional to the electric conductivity σ and therefore the conductivity effect could be sizable in the case of a weakly interacting QGP. However, the electric conductivity—as evaluated within PHSD in a finite box with periodic boundary conditions—is much lower and comparable to lattice QCD results for temperatures from 170–250 MeV. For more details and explicit comparisons we refer the reader to Ref. [23].

Now the question is: What is the maximal strength of this induced current and how to see that experimentally?

III. PHSD PREDICTIONS FOR THE DIRECTED FLOW IN Cu + Au COLLISIONS

It is widely recognized that fluctuations in the initial geometry of colliding nuclei are very important. At fixed impact parameter, depending on the location of the participant nucleons in the nucleus at the time of the collision, the actual shape of the overlap area may vary: the orientation and eccentricity of the ellipse defined by the participants fluctuates from event to event, i.e., the reaction plain fluctuates, too. We recall that taking into account these fluctuations in the initial geometry, the PHSD model reasonably describes the rapidity dependence $v_1(y)$ of the directed flow of charged hadrons including their slopes at midrapidity as well as the flow dependence on beam energy for symmetric Au + Au collisions [40].

Electromagnetic effects in particle emission clearly imply the dependence of specific observables on a particle charge, in particular also for particles of the same mass (e.g., π^+ and π^- mesons). For specific components of the electromagnetic field contributing to pion directed flow (different from that in asymmetric collisions), such a charge dependence (charge splitting) was predicted even for symmetric nuclear combinations in Refs. [22,25]. In a simplified treatment of Ref. [22] the effect is reduced to the relative distance between spectator blobs, which is a parameter to be fixed by data in order to achieve an agreement with a particular experiment and therefore it is not robust. The importance of precise experimental data on directed flows measured separately for positive and negative pion charges $v_1^{\pi+}, v_1^{\pi-}$ becomes clearly evident.

The results of the STAR Collaboration on the directed flow of protons, antiprotons, and pions in the Au + Au collision energy range from $\sqrt{s_{NN}} = 7.7$ up to 200 GeV have been recently published [6]. These data include measurements of v_1 for $p, \bar{p}, \pi^+$, and π^- for seven collision energies in the c.m.s. rapidity range of $|y| < 1$. The comparison of positive and negative pion directed flow at the $\sqrt{s_{NN}} = 7.7$ GeV (but not at higher energies) in intermediate centrality (10–40 %) Au + Au collisions displays a clear splitting of $v_1^{\pi+}$ and $v_1^{\pi-}$, with $v_1^{\pi+} < v_1^{\pi-}$ at positive rapidity. As noted in Ref. [25], this appears consistent with the expectation of a specific charge-dependent component of the directed flow induced by electromagnetic effects but this connection should be checked independently.

Similarly to the symmetric case, the directed flow of hadron distributions in asymmetric Cu + Au collisions is defined as

$$v_1 = \langle \cos(\phi - \Psi_{RP}) \rangle, \qquad (1)$$

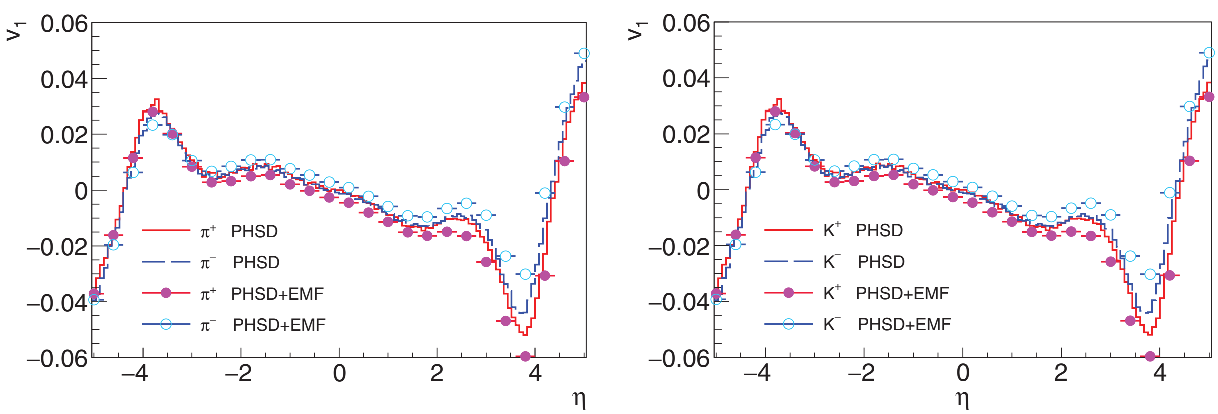

FIG. 3. (Color online) Rapidity dependence of the directed flow of pions and kaons created in off-central Cu + Au collisions at $\sqrt{s_{NN}} = 200$ GeV. The PHSD results for positive pions and kaons v_1^+ and for negative ones v_1^- are plotted by the solid and dashed histograms, respectively. Results by including the effect of the electromagnetic field on early charges are marked by filled and empty circles for v_1^+ and v_1^-, respectively.

TABLE I. The directed flow at mid-η, $v_1(\eta = 0)$, for Cu + Au ($\sqrt{s_{NN}} = 200$ GeV) collisions at $4.7 < b < 9.5$ fm.

hadron	$v_1(\eta = 0)$ PHSD	$v_1(\eta = 0)$ PHSD + EMF
π^+	$(-0.68 \pm 0.140) \times 10^{-3}$	$(-3.87 \pm 0.133) \times 10^{-3}$
π^-	$(-1.09 \pm 0.136) \times 10^{-3}$	$(1.71 \pm 0.129) \times 10^{-3}$
K^+	$(-1.37 \pm 0.312) \times 10^{-3}$	$(-6.33 \pm 0.311) \times 10^{-3}$
K^-	$(-2.11 \pm 0.327) \times 10^{-3}$	$(2.43 \pm 0.327) \times 10^{-3}$
p	$(-2.82 \pm 0.443) \times 10^{-3}$	$(-8.37 \pm 0.419) \times 10^{-3}$
$\bar{p}$	$(-1.58 \pm 0.504) \times 10^{-3}$	$(4.94 \pm 0.479) \times 10^{-3}$

where azimuthal angles ϕ are measured with respect to the transverse direction of the reaction plane Ψ_{RP}. Ideally, the reaction plane Ψ_{RP} is defined by the vector of the impact parameter and the beam direction. It is found that the magnitude of v_1 is correlated with the determination of the reaction plane. Here we associate Ψ_{RP} with the participants of the Au nucleus. For a comparison of v_1 distributions resulting from different definitions of the reaction plane we refer the reader to Ref. [27]. The results presented in Fig. 3 are calculated for identified $\pi^\pm$ and $K^\pm$ mesons taking into account the spectator electromagnetic field as well as its influence on quasiparticle transport in both partonic and hadronic phases. The filled and empty circles result from calculations that assume all partonic charges to be present immediately after string dissolution to partons. The dashed and solid histograms are obtained in the other scenario when the early electric acceleration is discarded or when the charges are delayed to their formation time and therefore appear together with the formation of the charged partons (quarks and antiquarks). These distributions as well as those presented below are calculated for the impact parameter range $4.7 \leqslant b \leqslant 9.5$ fm, which corresponds to (10–40 %) centrality. The number of simulated events amounts to 2×10^6 in the case of including the electromagnetic field and without it. The pseudorapidity dependence of v_1 exhibits a negative slope around mid-η. In addition, $v_1(\eta)$ displays a dipolelike asymmetry between the forward and backward rapidity distributions. The magnitude of v_1 at the forward pseudorapidity (the Au-like side) is higher than that at the backward one (the Cu-like side). Due to this nuclear asymmetry the pseudorapidity dependence of $v_1(\eta)$ for every hadron does not go through zero at midrapidity ($\eta = 0$), as follows from Table I. All the slopes at this point $dv_1/d\eta(\eta = 0)$ are negative and small as presented in Table II. An even

TABLE II. Estimated slope parameters $dv_1/d\eta(\eta = 0)$ for Cu + Au ($\sqrt{s_{NN}} = 200$ GeV) collisions at $4.7 < b < 9.5$ fm. Parameters of the η distributions are defined by a linear fit for $|\eta| < 0.7$.

hadron	$dv_1/d\eta$ PHSD	$dv_1/d\eta$ PHSD + EMF
π^+	$(-5.26 \pm 0.340) \times 10^{-3}$	$(-6.39 \pm 0.299) \times 10^{-3}$
π^-	$(-5.68 \pm 0.330) \times 10^{-3}$	$(-6.18 \pm 0.291) \times 10^{-3}$
K^+	$(-5.28 \pm 0.751) \times 10^{-3}$	$(-4.97 \pm 0.750) \times 10^{-3}$
K^-	$(-6.24 \pm 0.789) \times 10^{-3}$	$(-7.26 \pm 0.789) \times 10^{-3}$
p	$(-14.9 \pm 1.07) \times 10^{-3}$	$(-6.39 \pm 0.299) \times 10^{-3}$
$\bar{p}$	$(-3.83 \pm 1.22) \times 10^{-3}$	$(-6.18 \pm 0.291) \times 10^{-3}$

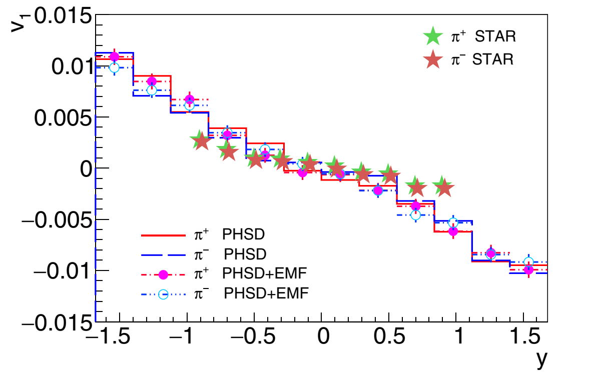

FIG. 4. (Color online) Rapidity dependence of the pion directed flow in Au + Au collisions at $\sqrt{s_{NN}} = 200$ GeV. The solid histogram is calculated in PHSD for π^+ and the dashed one for π^- mesons. Results from PHSD by including the effect of the electromagnetic field on early charges are marked by filled and empty circles for v_1^+ and v_1^-, respectively. Experimental data points (stars) are from Ref. [6].

stronger charge asymmetry of v_1 in forward and backward rapidities is seen at larger pseudorapidity ($|\eta| \geqslant 2.5$), with the magnitude of v_1 at large backward pseudorapidity (Cu-like rapidity) being lower than that at large forward pseudorapidity (Au-like rapidity).

In Fig. 4 the directed π^+ $v_1^{\pi^+}(y)$ and π^- $v_1^{\pi^-}(y)$ flows from PHSD are contrasted to the symmetric Au + Au case. As is seen there is practically no dependence of the $v_1(y)$ distributions on the pion charge as well as on the electromagnetic field. Note that similar PHSD results have been obtained earlier for the same colliding system from the analysis of elliptic flow [31]. In agreement with this finding, the π^+ and π^- meson spectra measured in Au + Au collisions coincide with each other [6]. Accordingly, the charge-dependent asymmetry of the directed flow in Cu + Au collisions originates from the electric field asymmetry induced by the asymmetry in charge of the initial colliding nuclei but not as a particularity of the observable under consideration.

The rapidity dependence of the directed flow $v_1(\eta)$ for $p/\bar{p}$ is presented in Fig. 5. For antiprotons, the $v_1(\eta)$

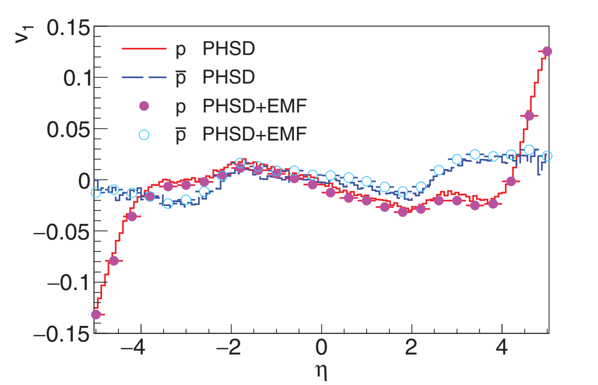

FIG. 5. (Color online) Rapidity dependence of the directed flow of protons and antiprotons in Cu + Au collisions at $\sqrt{s_{NN}} = 200$ GeV. The notation is the same as in Fig. 3.

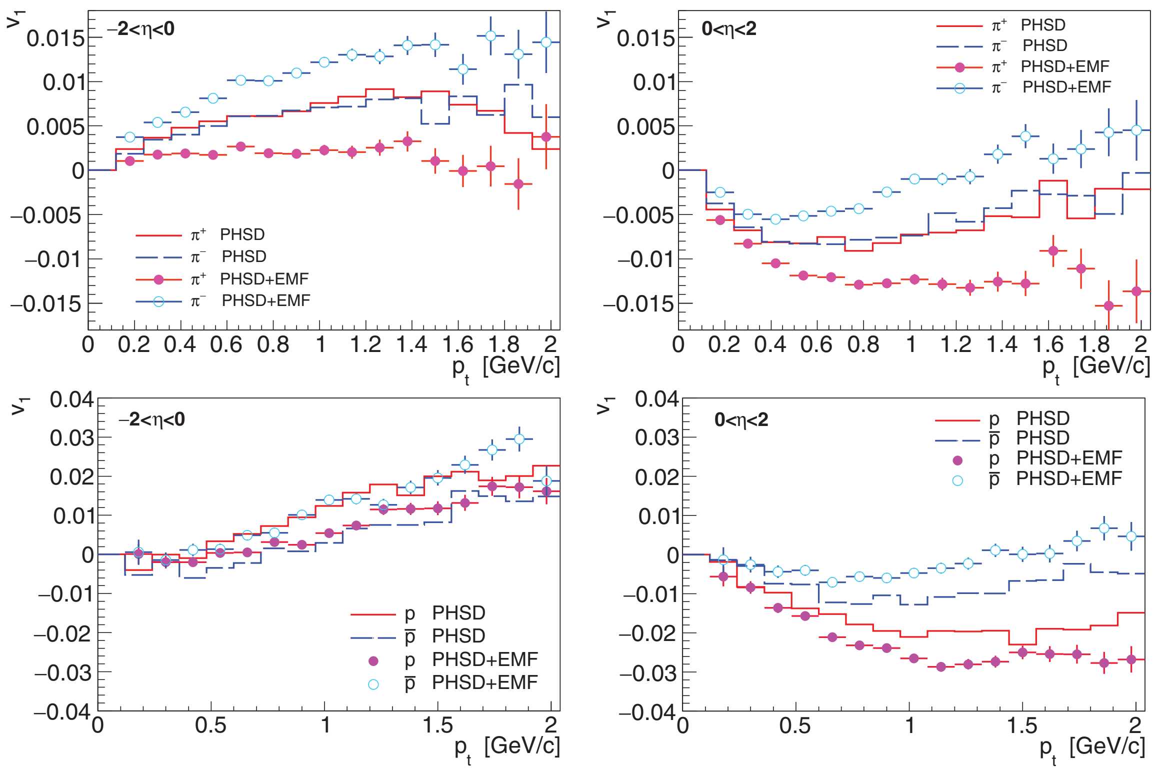

FIG. 6. (Color online) Transverse momentum dependence of the directed flow for $\pi^{\pm}$ (top) and protons and antiprotons (bottom) produced in peripheral Cu + Au collisions for forward (right) and backward (left) emitted hadrons at $\sqrt{s_{NN}} = 200$ GeV. The notation is the same as in Fig. 3.

is comparatively flat with a weak increase towards large pseudorapidities. The proton and antiproton results are close to each other at $|\eta| \lesssim 2.5$ but strongly differ at higher rapidities due to contributions from the fragmentation process. The shape of the proton directed flow distribution $v_1(\eta)$ resembles that for the created mesons (cf. Fig. 3) since the mesons and baryons/antibaryons emerge dominantly by hadronization from the same partonic medium. One should note that the observed differences between the directed flow of protons and antiprotons could give information also on the different rate of baryon stopping on the Cu and Au side of the fireball. Moreover, the reaction plane correlations in the fireball are modified in asymmetric collisions with stronger correlations between odd- and even-order event planes [41,42].

Figure 6 shows the PHSD results for transverse momentum distributions of the directed flow. It is seen that the $v_1(p_T)$ functions for π^+ and π^- mesons coincide with each other if electromagnetic forces are neglected (histograms in the top panel of Fig. 6) or if partonic charges appear only after $t \geqslant 0.5$ fm/c. In this case the v_1^{π} is negative in the forward direction and positive at negative angles $-2 < \eta < 0$. The inclusion of the early electromagnetic field noticeably changes these p_T distributions increasing v_1 for negative pions and decreasing v_1 for positive pions. In both cases the splitting effect is clearly seen but the shape of $v_1^{\pi}(p_T)$ also depends on the pion electric charge and pseudorapidity interval. For the backward π^- emission the directed flow v_1 grows monotonically with momentum while $v_1^{\pi+}(p_T) \approx 0$ for $p_T \lesssim 1.4$ GeV and then decreases with p_t. As to the forward angles $0 \leqslant \eta \leqslant 2$, the directed flow v_1^- increases also but exhibits a wide negative minimum in the region of $p_T \approx 0.3$–0.5 GeV/c. The directed flow of positive pions is seen to decrease and then to flatten at $p_T \geqslant 1$ GeV/c, being negative in the whole transverse momentum range.

The directed flow $v_1(p_T)$ for protons and antiprotons shown in Fig. 6 (bottom) displays a strong asymmetry in the forward and backward pseudorapidities, having a larger $v_1(p_T)$ splitting at forward (the Cu side) pseudorapidity than that at backward (the Au side) pseudorapidity. Note that even without taking into account the electromagnetic effect there is a difference in v_1 between p and $\bar{p}$ due to different interaction mechanisms of these hadrons (see bottom panels in Fig. 6). In the baryonic case the influence of the created electromagnetic field is not so large as for pions and is more easily seen in the forward direction $0 \leqslant \eta \leqslant 2$. The momentum dependence of $v_1(p_T)$ in the backward direction is a positive monotonously increasing function but in the forward direction $v_1(p_T) \lesssim 0$ with a weak wide minimum at $p_T \sim 0.7$ GeV/c for the case of antiprotons. The distribution $v_1(p_T)$ for protons is similar to that for π^+: it decreases till $p_T \sim 1$ GeV/c and then flattens.

We finally note in passing that when including also the electromagnetic fields as induced by participant charges in addition to those discussed before, the control PHSD calculations ($\sim 1.5 \times 10^5$ events) on the charge-dependent directed flow presented in this work only change within the statistical accuracy.

IV. CONCLUSIONS

Asymmetric Cu + Au collisions have been studied at the ultrarelativistic energy $\sqrt{s_{NN}} = 200$ GeV within the PHSD approach, which is in a reasonable agreement with available experimental data for symmetric Au + Au collisions in the energy range from the SPS to the top RHIC energy. The retarded electromagnetic field induced by spectator protons has been calculated (and quantified) and its influence on the quasiparticle transport has been taken into account within two model scenarios: (i) if the initial field energy at times $\sim$0.1 fm/c after contact is dominantly carried by (still unformed) charged quarks and antiquarks and (ii) if the quark/antiquark creation (and accordingly the presence of electric charges) is delayed to their formation time.

Independent of the two scenarios we have explicitly demonstrated that in peripheral collisions of Cu + Au an additional short-time electric field eE_x in the direction of the lighter nucleus emerges which at top RHIC energies is essentially effective for the first 0.25 fm/c and is due to the asymmetry in the number of protons in the target and projectile nuclei. This additional electric field is not present in symmetric Au + Au collisions but can be used in asymmetric collisions to study the electric response of the medium during the passage time of the nuclei, i.e., also out of equilibrium. In fact, the detailed PHSD predictions for the charge differential directed flow $v_1(\eta, p_t)$ in Cu + Au reactions show that the scenario (i) leads to clearly observable effects in the directed flow of hadrons with the same masses but different electric charges, for example $\pi^+ - \pi^-$, $K^+ - K^-$, $p - \bar{p}$. These differences can be studied by means of the charge-dependent pseudorapidity dependence of $v_1(\eta)$. High-precision data on the transverse momentum dependence $v_1(p_t)$, furthermore, should clarify the situation and differentiate between the two scenarios because in case of ii) there are almost no early electric charges of low p_t and accordingly no effects from the early electric acceleration.

The experimental observation of the splitting effect in charge-dependent observables of the direct flow would be a direct confirmation of the importance of electromagnetic fields in relativistic heavy-ion collision dynamics and might shed further light on the effective degrees of freedom in the very early nonequilibrium phase and possibly also on the photon v_2 puzzle [43].

ACKNOWLEDGMENTS

We are grateful to E. L. Bratkovskaya and V. P. Konchakovski for useful discussions. V.T. and V.V. acknowledge the Heisenberg-Landau grant support and support within the HIC for FAIR framework. The work of S.V. is supported by the U.S. Department of Energy Office of Science, Office of Nuclear Physics under Award No. DE-FG02-92ER-40713.

[1] S. A. Voloshin, A. M. Poskanzer, and R. Snellings, in *Landolt-Boernstein New Series*, I/23, edited by R. Stock (Springer-Verlag, Berlin, 2010), pp. 5–54.
[2] P. Sorensen, in *Quark-Gluon Plasma 4*, edited by R. Hwa and X. N. Wang (World Scientific, Singapore, 2010).
[3] A. Peshier and W. Cassing, Phys. Rev. Lett. **94**, 172301 (2005); M. Gyulassy and L. McLerran, Nucl. Phys. A **750**, 30 (2005).
[4] W. Reisdorf and H. G. Ritter, Annu. Rev. Nucl. Part. Sci. **47**, 663 (1997).
[5] N. Herrmann, J. P. Wessels, and T. Wienold, Ann. Rev. Nucl. Part. Sci. **49**, 581 (1999).
[6] L. Adamczyk *et al.* (STAR Collaboration), Phys. Rev. Lett. **112**, 162301 (2014).
[7] V. P. Konchakovski, W. Cassing, Yu. B. Ivanov, and V. D. Toneev, Phys. Rev. C **90**, 014903 (2014).
[8] Yu. B. Ivanov, V. N. Russkikh, and V. D. Toneev, Phys. Rev. C **73**, 044904 (2006).
[9] D. H. Rischke, Nucl. Phys. A **610**, 88 (1996).
[10] H. Stöcker, Nucl. Phys. A **750**, 121 (2005).
[11] L.-W. Chen and C. M. Ko, Phys. Rev. C **73**, 014906 (2006).
[12] P. Bozek, Phys. Lett. B **717**, 287 (2012).
[13] B. Schenke, P. Tribedy, and R. Venugopalan, arXiv:1403.2232.
[14] A. Iordanova (for the PHENIX Collaboration), J. Phys.: Conf. Ser. **458**, 012004 (2013); H. Nakagomi, Riken Rad. Lab. Meeting, 2014 (unpublished).
[15] D. Teaney and L. Yan, Phys. Rev. C **83**, 064904 (2011).
[16] M. Luzum and J.-Y. Ollitrault, Phys. Rev. Lett. **106**, 102301 (2011).
[17] Md. Rihan Haque, M. Nasim, and B. Mohanty, Phys. Rev. C **84**, 067901 (2011).
[18] P. Bozek and I. Wyskiel, Phys. Rev. C **81**, 054902 (2010).
[19] R. Andrade, A. Reis, F. Grassi, Y. Hama, T. Kodama and J. Y. Ollitrault and W. L. Qian, Indian J. Phys. **84**, 1657 (2011).
[20] S. Huang, arXiv:1210.5570.
[21] A. Iordanova, RHIC & AGS Annual User's Meeting: Workshop on U-U and Cu-Au studies, 2014 (unpublished).
[22] Y. Hirono, M. Hongo, and T. Hirano, Phys. Rev. C **90**, 021903 (2014).
[23] W. Cassing, O. Linnyk, T. Steinert, and V. Ozvenchuk, Phys. Rev. Lett. **110**, 182301 (2013); T. Steinert and W. Cassing, Phys. Rev. C **89**, 035203 (2014).
[24] A. Rybicki and A. Szczurek, arXiv:1405.6860; Phys. Rev. C **87**, 054909 (2013); **75**, 054903 (2007).
[25] U. Gürsoy, D. Kharzeev, and K. Rajagopal, Phys. Rev. C **89**, 054905 (2014).
[26] V. Voronyuk, V. D. Toneev, W. Cassing, E. L. Bratkovskaya, V. P. Konchakovski, and S. A. Voloshin, Phys. Rev. C **83**, 054911 (2011).
[27] J. Wang, Y.-G. Ma, G.-Q. Zhang, and W.-Q. Shen, arXiv:1411.1812.
[28] S. Juchem, W. Cassing, and C. Greiner, Phys. Rev. D **69**, 025006 (2004); Nucl. Phys. A **743**, 92 (2004).
[29] W. Cassing and E. L. Bratkovskaya, Nucl. Phys. A **831**, 215 (2009); Phys. Rev. C **78**, 034919 (2008); W. Cassing, Nucl. Phys. A **791**, 365 (2007).
[30] W. Cassing, E. Phys. J. ST **168**, 3 (2009).
[31] V. P. Konchakovski, E. L. Bratkovskaya, W. Cassing, V. D. Toneev, and V. Voronyuk, Phys. Rev. C **85**, 011902 (2012).
[32] O. Linnyk, E. L. Bratkovskaya, V. Ozvenchuk, W. Cassing, and C. M. Ko, Phys. Rev. C **84**, 054917 (2011); O. Linnyk,

W. Cassing, J. Manninen, E. L. Bratkovskaya, and C. M. Ko, *ibid.* **85**, 024910 (2012); O. Linnyk, W. Cassing, J. Manninen, E. L. Bratkovskaya, P. B. Gossiaux, J. Aichelin, T. Song, and C. M. Ko, *ibid.* **87**, 014905 (2013); O. Linnyk, V. P. Konchakovski, W. Cassing, and E. L. Bratkovskaya, *ibid.* **88**, 034904 (2013).
[33] V. D. Toneev *et al.*, Phys. Rev. C **85**, 034910 (2012).
[34] W. Ehehalt and W. Cassing, Nucl. Phys. A **602**, 449 (1996).
[35] W. Cassing and E. L. Bratkovskaya, Phys. Rep. **308**, 65 (1999).
[36] W. Cassing, E. L. Bratkovskaya, and S. Juchem, Nucl. Phys. A **674**, 249 (2000).
[37] A. Bzdak and V. Skokov, Phys. Lett. B **710**, 171 (2012).
[38] W.-T. Deng and X.-G. Huang, Phys. Rev. C **85**, 044907 (2012).
[39] K. Tuchin, Int. J. Mod. Phys. E **23**, No. 1, 1430001 (2014).
[40] V. P. Konchakovski, E. L. Bratkovskaya, W. Cassing, V. D. Toneev, S. A. Voloshin, and V. Voronyuk, Phys. Rev. C **85**, 044922 (2012).
[41] P. Bozek, W. Broniowski, and J. Moreira, Phys. Rev. C **83**, 034911 (2011).
[42] R. S. Bhalerao, M. Luzum, and J.-Y. Ollitrault, Phys. Rev. C **84**, 054901 (2011).
[43] E. L. Bratkovskaya, arXiv:1408.3674; O. Linnyk, W. Cassing, and E. L. Bratkovskaya, Phys. Rev. C **89**, 034908 (2014).